

A plasma membrane-bound putative endo-1,4- β -D-glucanase is required for normal wall assembly and cell elongation in *Arabidopsis*

Frédéric Nicol¹, Isabelle His²,
Alain Jauneau², Samantha Vernhettes¹,
Hervé Canut³ and Herman Höfte^{1,4}

¹Laboratoire de Biologie Cellulaire, Institut National de Recherche Agronomique, Route de Saint-Cyr, F-78026 Versailles Cedex,

²Université de Rouen, CNRS UPRESA 6307, Faculté des Sciences, F-76821 Mont-Saint-Aignan Cedex and ³Centre de Physiologie Végétale de l'Université Paul Sabatier, U.A. CNRS No. 241, 118, Route de Narbonne, F-31062 Toulouse Cedex, France

⁴Corresponding author

Endo-1,4- β -D-glucanases (EGases) form a large family of hydrolytic enzymes in prokaryotes and eukaryotes. In higher plants, potential substrates *in vivo* are xyloglucan and non-crystalline cellulose in the cell wall. Gene expression patterns suggest a role for EGases in various developmental processes such as leaf abscission, fruit ripening and cell expansion. Using *Arabidopsis thaliana* genetics, we demonstrate the requirement of a specialized member of the EGase family for the correct assembly of the walls of elongating cells. *KORRIGAN* (*KOR*) is identified by an extreme dwarf mutant with pronounced architectural alterations in the primary cell wall. The *KOR* gene was isolated and encodes a membrane-anchored member of the EGase family, which is highly conserved between mono- and dicotyledonous plants. *KOR* is located primarily in the plasma membrane and presumably acts at the plasma membrane–cell wall interface. *KOR* mRNA was found in all organs examined, and in the developing dark-grown hypocotyl, mRNA levels were correlated with rapid cell elongation. Among plant growth factors involved in the control of hypocotyl elongation (auxin, gibberellins and ethylene) none significantly influenced *KOR*-mRNA levels. However, reduced *KOR*-mRNA levels were observed in *det2*, a mutant deficient for brassinosteroids. Although the *in vivo* substrate remains to be determined, the mutant phenotype is consistent with a central role for *KOR* in the assembly of the cellulose–hemicellulose network in the expanding cell wall.

Keywords: cell elongation/cell wall/cellulose/endo-1,4- β -D-glucanase/xyloglucan

Introduction

Endo-1,4- β -D-glucanases (EGases) constitute a large, ubiquitous family of enzymes that hydrolyse 1,4- β linkages adjacent to unsubstituted glucose residues (Henrissat *et al.*, 1989; Brummell *et al.*, 1994). Microbial EGases can degrade crystalline cellulose, and are intensively studied and used in industrial processes. Plant EGases form a separate subclass (type E2, Brummell *et al.*, 1994), lack

a cellulose-binding domain and are unable to hydrolyse crystalline cellulose. *In vitro* activity has been observed with various 1,4- β -linked glucan polymers such as xyloglucans or the artificial substrate carboxy-methyl cellulose (CMC). However, the *in vivo* substrates remain to be determined. All higher plant species investigated express multiple EGases, for instance in *Arabidopsis thaliana* at least a dozen different family members can be found in sequence databases (F.Nicol and H.Höfte, unpublished data). It is not known to what extent different family members vary in their biochemical properties. The expression of most plant EGases is tightly regulated, suggesting a role in plant development. Some EGases are expressed specifically during fruit ripening or leaf abscission (Cass *et al.*, 1990; Tucker and Milligan, 1991; Lashbrook *et al.*, 1994; Ferrarese *et al.*, 1995; Del Campillo and Bennett, 1996). The expression of other EGases is highest in expanding cells which may be indicative of a role in cell wall polysaccharide assembly or rearrangements in the primary cell wall. A role for EGases in cell expansion has been debated over the past 20 years, and despite the vast body of literature, the issue remains controversial (Hoson and Nevins, 1989; Inouhe and Nevins, 1991; Wu *et al.*, 1996; Brummell *et al.*, 1997).

To understand the mechanism of plant cell expansion, it should be noted that plant cells are surrounded by a polymeric cell wall which imposes constraints on the cell expansion process. The wall must resist the extreme tensile forces exerted by the osmotic pressure of the protoplast and at the same time, in a growing cell, it must be able to expand in a coordinated fashion without losing its integrity. Wall expansion involves an initial stress relaxation (Cosgrove, 1997), followed by the biosynthesis of new polymers and their regulated incorporation into the wall structure. The molecular mechanisms underlying these processes are poorly understood. Primary cell walls of dicotyledonous plants are composed of three major classes of polysaccharides: cellulose, xyloglucan and pectin (Carpita and Gibeau, 1993). Cellulose microfibrils are composed of 1,4- β -D-glucan polymers synthesized by putative cellulose–synthase complexes which can be visualized as rosettes on freeze–fracture images of the plasma membrane. Genes encoding the catalytic subunit of cellulose synthase were recently identified in cotton and *A.thaliana* (Pear *et al.*, 1996; Arioli *et al.*, 1998).

The matrix polysaccharides, xyloglucans and pectins, are synthesized in the Golgi apparatus and secreted into the cell wall (Staehelin and Moore, 1995). Since the biosynthetic enzymes have not been purified nor the genes cloned, little is known about their biosynthesis. Also, the mechanisms regulating synthesis and secretion of matrix polysaccharides during cell expansion remain largely unknown. Upon release into the apoplast, xyloglucans bind tightly to the nascent cellulose microfibrils through

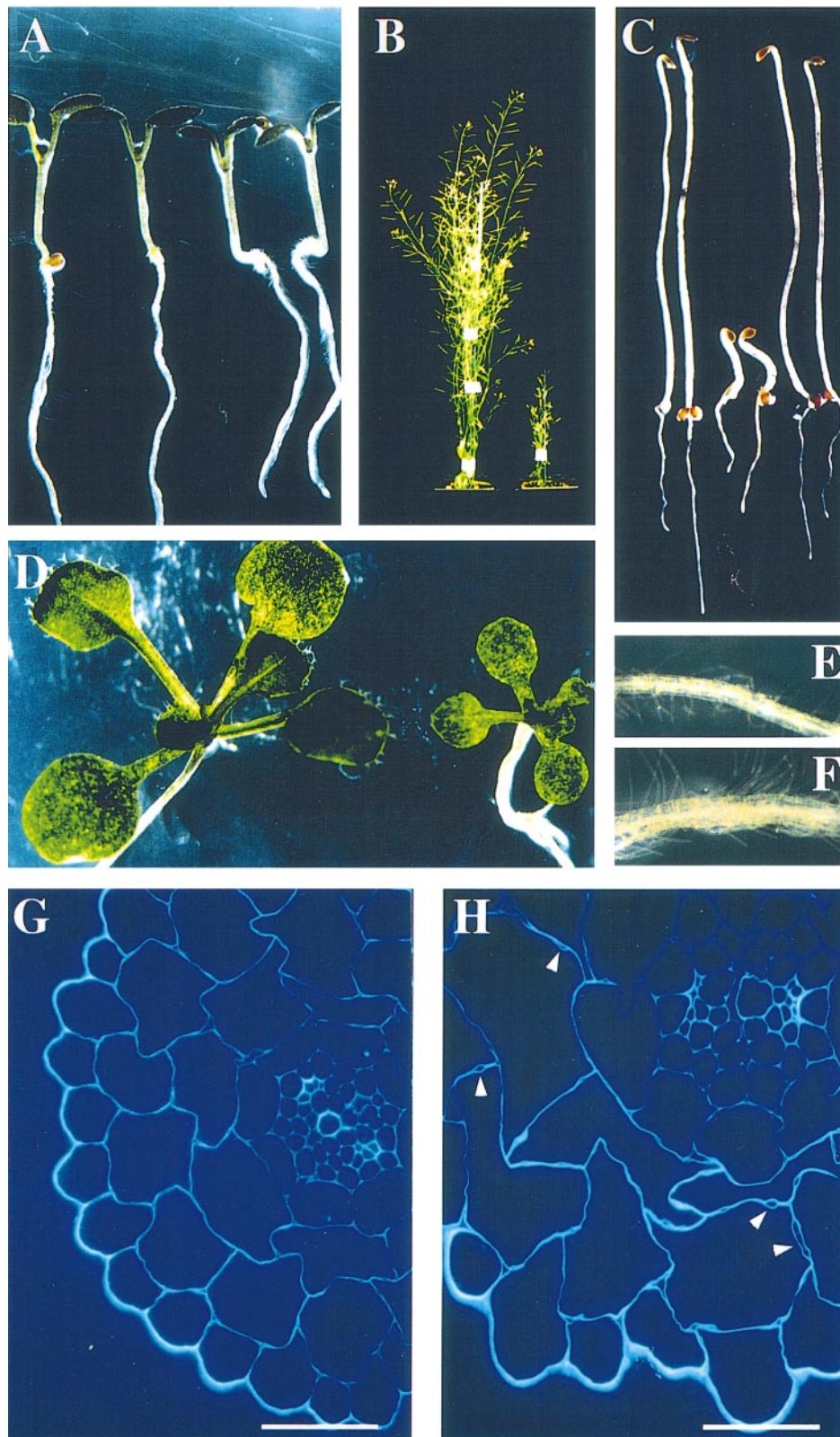


Fig. 1. *kor* mutant phenotype. (A) Seven-day-old light-grown wild-type (left) and *korrigan* (right) seedlings. (B) Six week-old greenhouse-grown plants: wild-type (left) and *korrigan* (right). (C) Seven-day-old dark-grown wild-type (left), *korrigan* (middle) and *kor* transformed with the 8.5 kb complementing genomic fragment (right) seedlings. (D) Fifteen-day-old light-grown wild-type (left) and *korrigan* (right) seedlings. (E) Seven-day-old light-grown wild-type roots. (F) Seven-day-old light-grown *korrigan* roots. Calcofluor-stained transverse sections through hypocotyls of 7-day-old dark-grown (G) wild-type and (H) *korrigan* seedlings. Arrows indicate wall separations often observed in the *kor* mutant. Scale bar represents 65 μ m.

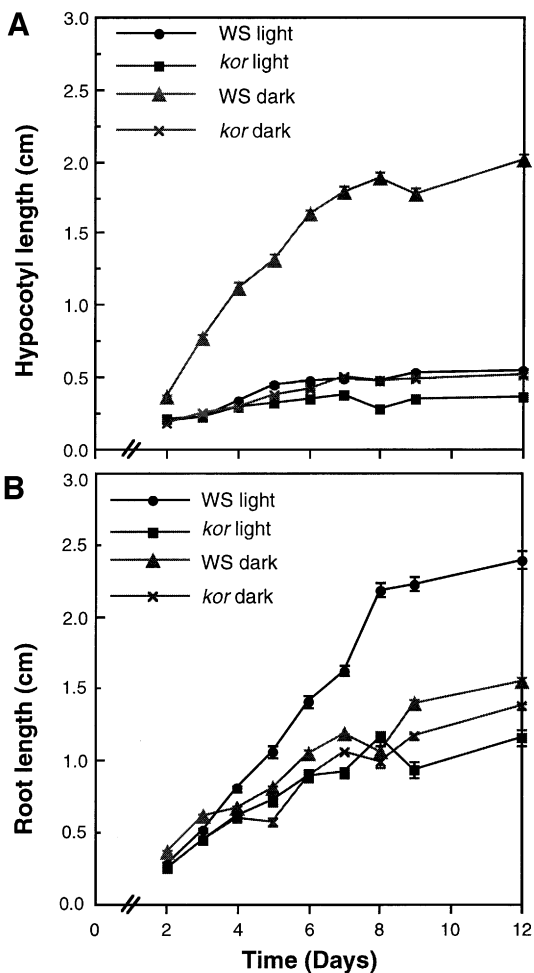


Fig. 2. Reduced hypocotyl and root growth in *kor* mutants. (A) Hypocotyl and (B) root lengths were measured as a function of the number of days after transfer to the growth chamber.

hydrogen bonds (Hayashi and Maclachlan, 1984; Hayashi, 1989). Electron microscopic evidence indicates that xyloglucan molecules form cross-bridges between cellulose microfibrils, thereby establishing a load-bearing cellulose-xyloglucan network (McCann *et al.*, 1990). Studies on tomato cell cultures adapted to the inhibitor of cellulose deposition, 2,6-dichlorobenzonitrile (DCB), indicate that cellulose-hemicellulose on the one hand, and pectins on the other hand, form two independent networks in the primary wall. DCB-adapted cell walls have greatly reduced cellulose contents. As a result, xyloglucans cannot bind to cellulose and are secreted into the medium. Surprisingly, in the absence of a cellulose-hemicellulose network, the wall integrity and strength is maintained by a Ca^{2+} -linked network of acidic pectins, as shown by the extreme susceptibility of these walls to Ca^{2+} -chelators.

Wall stress relaxation may involve slippage or hydrolysis of the load-bearing xyloglucan cross-bridges (Cleland, 1971; Albersheim, 1975; Hayashi and Maclachlan, 1984) and it has frequently been suggested that EGases, together with other cell-wall proteins, such as expansins and xyloglucan-endo-transglycosylases, may play a role in this process.

To our knowledge, this work represents the first demonstration of an essential role for a member of the EGase

family in plant cell expansion. The gene was cloned from an *A.thaliana* dwarf mutant, *korrigan* (*kor*), showing a defect in the elongation of all non-tip-growing cells examined. *KOR* encodes an evolutionarily conserved integral membrane protein which is primarily located in the plasma membrane. *KOR*-transcript levels in the hypocotyl correlated positively with cell elongation and were not affected in mutants overproducing free auxin or ethylene, or mutants deficient in gibberellins. In contrast, a mutant deficient in brassinosteroids showed reduced *KOR*-mRNA levels. The observed structural alterations in the mutant cell wall suggest a role for *KOR* in the correct assembly of the cellulose-hemicellulose network in the expanding cell wall.

Results

kor, a novel cell elongation mutant

kor was found as a single allele in a screen for short hypocotyl mutants among dark-grown T-DNA or chemically mutagenized seedlings. Despite the relatively large scale of the screen, no other alleles for *KOR* were identified although several alleles were found for other loci like *PROCUSTE* (eight alleles, H.Höfte, unpublished data and Desnos *et al.*, 1996) and *BOTERO* (six alleles, H.Höfte, unpublished data).

The segregation in the progeny of *kor* heterozygous plants showed a 3:1 ratio (1136 wild-type and 386 *kor* seedlings among 1522 seeds sown; $\chi^2 = 0.031$; $P < 0.05$) which demonstrates that the mutant phenotype segregates as a single, recessive, nuclear locus.

The genetic map position of the locus was deduced from the localization of the cloned *KOR* gene (see below) on two yeast artificial chromosomes (CIC4G5 and CIC8D5) containing the microsatellite marker nga129, which maps to the bottom of chromosome V (position 81.7).

The hypocotyl of 7-day-old dark-grown *kor* seedlings was four times shorter (Figures 1C and 2A) than that of the wild-type, but elongation kinetics were unchanged. For both the mutant and wild-type, the hypocotyl elongated between day 2 and 7, after which a plateau was reached (Figure 2A). *kor* hypocotyls grown in white light were only slightly shorter than those of the wild-type (Figures 1A and 2A). Root growth was also reduced in the mutant compared with wild-type (Figures 1C and 2B) and the difference was most pronounced in the light. In light conditions the root growth rate of the wild-type was significantly higher (0.19 cm/day) than in dark-grown plants (0.12 cm/day). The size of all other organs investigated was also reduced in *kor*, including stems, rosette leaves, flowers and siliques (Figure 1B and D). Despite the reduced size, mutant plants were fully fertile. No differences in size between the mutant and wild-type were observed for tip-growing cells such as trichomes and root hairs (data not shown). Furthermore, the normal Mendelian segregation ratio for the mutant phenotype suggested that pollen tube elongation was unaffected.

Scanning electron microscopy (SEM) of mutant dark-grown hypocotyls revealed an irregular surface (Figure 3J) consisting of epidermal cells with irregular shapes. Wide cells alternated with narrow cells and some cells had collapsed entirely or had failed to expand. Although

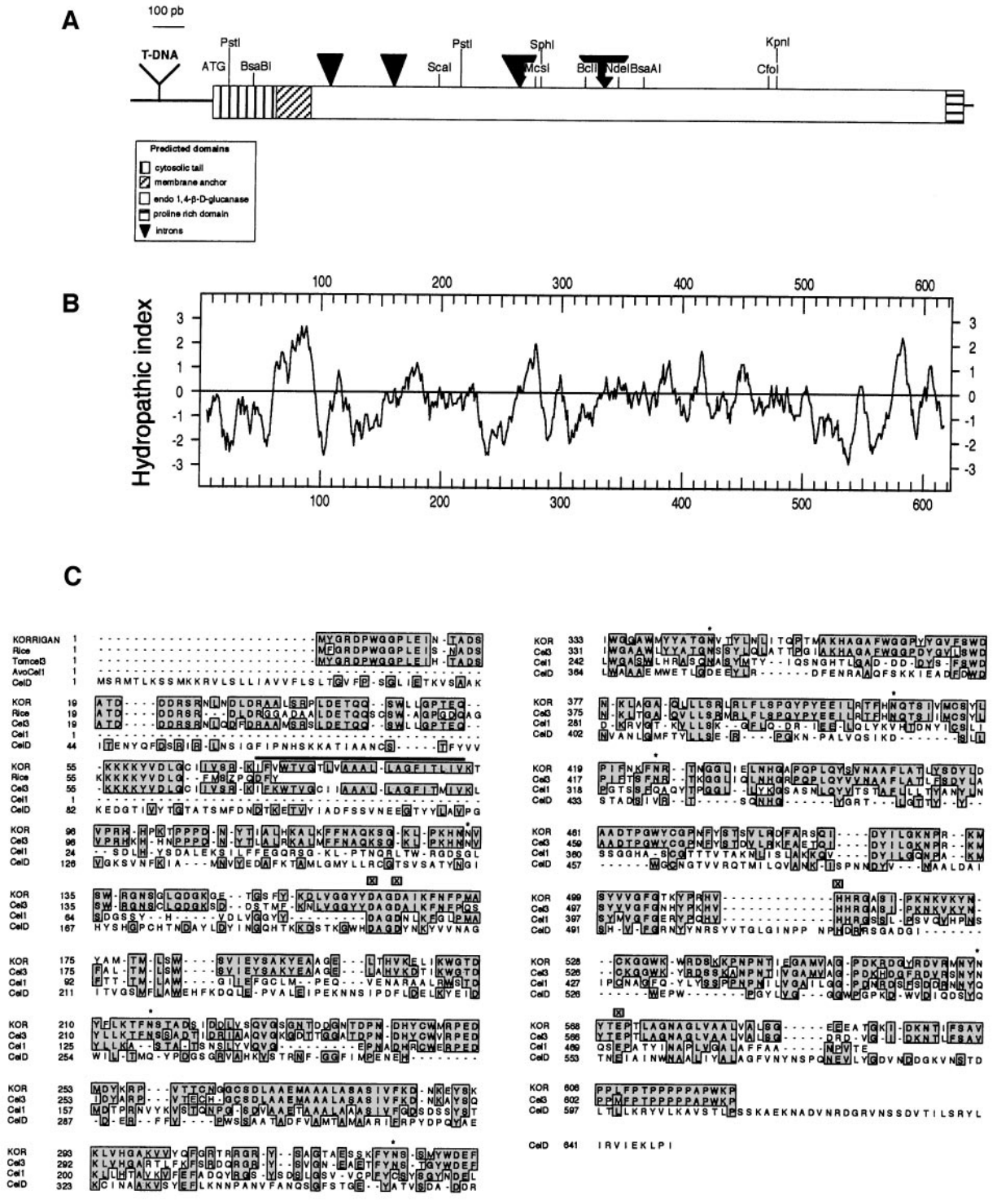


Fig. 4. KOR, a putative membrane-bound endo-1,4-β-D-glucanase. (A) Domain structure: unique restriction sites in the gene sequence are shown, introns are represented by black arrows, the T-DNA is inserted 200 bp upstream of the ATG-initiation codon. The predicted N-terminal cytosolic tail, the membrane anchor and the extracellular EGase domain and the proline-rich C-terminal domain are indicated. (B) Hydropathicity plot according to Kyte and Doolittle (1982). (C) Alignment of KOR with plant and bacterial EGases: AvoCel1, Tomcel3 and celD are the amino acids sequences of a soluble EGase from avocado without the signal peptide, a membrane-bound EGase from tomato, an EGase from *Clostridium thermocellum*, respectively. The predicted amino acid sequence of a rice EST is included. ☒ represents the residues essential for catalytic activity identified in celD which are also conserved in KOR (Asp198, Asp201, H516, Glu555); * indicates the eight predicted glycosylation sites. The thick black line overlies the predicted transmembrane domain in KOR (Von Heijne, 1986). The accession numbers are as in Figure 5.

several enzymes and probed with DNA fragments corresponding to either the left or right T-DNA border revealed a single, simple T-DNA insertion. Plant DNA flanking the

right border was isolated and used to obtain genomic clones. Complementation tests were carried out with an 8.5 kb DNA fragment, presumably containing the entire

gene, cloned into a binary T-DNA vector carrying a hygromycin-resistance gene. Plants heterozygous for *kor* were transformed by *in planta* infiltration (Bechtold *et al.*, 1993). All primary transformants had a wild-type phenotype in the light. The T₂ progeny obtained after selfing of one of these transformants segregated for *kor* with a 1:15 ratio (65 *kor* and 1167 wild-type seedlings of 1232 seeds sown; $\chi^2 = 0.12$; $P < 0.05$) which was expected for an unlinked insertion complementing the mutant phenotype. In addition, all phenotypically mutant T₂ seedlings were hygromycin-sensitive, whereas all hygromycin-resistant seedlings had a wild-type phenotype in the light and in the dark. The transformation efficiency of plants homozygous for *kor* was much less efficient and yielded only a single transformant. This transformant showed a wild-type phenotype. The T₂ progeny from this transformant was 100% kanamycin-resistant, confirming the homozygous state of the T-DNA tagged *kor* mutation, and segregated the wild-type phenotype in a 3:1 ratio (315 wild-type and 95 *kor* seedlings of 410 seeds sown; $\chi^2 = 0.75$; $P < 0.05$). All wild-type plants were also hygromycin resistant, indicating the presence of the transgene. Figure 1C shows that the presence of one copy of the transgene completely restores the phenotype of dark-grown seedlings homozygous for the *kor* mutation to wild-type. The adult phenotype was also entirely complemented in the transformant (data not shown). All these data indicate that the 8.5 kb fragment had complemented the mutation and therefore should contain the *KOR* gene.

A 2.3 kb cDNA clone was isolated using the right border T-DNA flanking fragment, and the sequence was compared with 3 kb of genomic sequence flanking the right border (DDJB/EMBL/GenBank accession No. AF073875). The genomic sequence contained five Open Reading Frames (ORFs) corresponding to the cDNA sequence interrupted by four introns (Figure 4A) with consensus splice-donor and acceptor sites. The first ATG codon is most likely to be the initiator codon, since it is preceded by an in-frame stop codon at -46 bp. The T-DNA is inserted 200 bp upstream of the initiator ATG, presumably in the promoter. The cDNA sequence is 100% identical to an *A.thaliana* sequence present in the public databases (DDJB/EMBL/GenBank accession No. U37702). The predicted amino acid sequence of 622 residues contains eight potential N-glycosylation sites and is similar over almost its entire length to EGases from plants and bacteria. For instance, the amino acid sequence is 43.3% identical to avocado Cel1 sequence and 44.4% identical to pea EGL1. In the bacterial enzyme CelD, site-directed mutagenesis and chemical modification techniques have identified four amino acids (D198/201, H516 and E555) as being potentially important in catalysis (Chauvaux *et al.*, 1992). As in other plant EGases, these four residues are also conserved in the KOR sequence (Figure 4C). KOR is highly similar (81.8% identity) to Cel3, a recently identified membrane-bound EGase family member in tomato (Brummel *et al.*, 1997). In contrast to all other plant EGases, the sequences of KOR and Cel3 do not contain a predicted cleavable signal peptide. Instead, the mature protein is predicted to be a type II integral membrane protein anchored in the membrane by a stretch of highly hydrophobic amino acids located in the N-terminus (Von

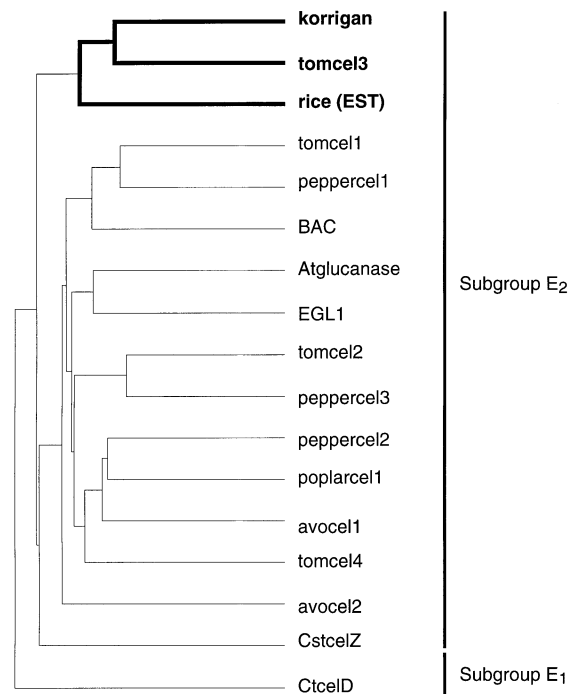


Fig. 5. KOR represents a distinct, evolutionarily conserved subclass of plant EGases. Similarity tree (Genetics Computer Group- version 9.0) of type E EGases after removal of the predicted signal sequences. This family consists of two subgroups whereby subgroup E2 possesses both microbial and plant members. Sequences and DDJB/EMBL/GenBank accession numbers are: *korriigan* (U37702), *tomcel3* (X97189), *rice* (EST; D46633), *tomcel1* (U13054), *pepper cell1* (X87323), *BAC* (M57400), *Atglucanase* (U17888), *EGL1* (L41046), *tomcel2* (U13055), *peppercel3* (X83711), *peppercel2* (X97190), *poplarcel1* (D32166), *avocel1* (M17634), *tomcel4* (U20590), *avocel2* (X55790), *CstcelZ* (X55299) and *CtcelD* (X04584).

Heijne, 1986; Figure 4A and B). The N-terminal stretch of 100 amino acids distinguishes KOR and Cel3 from other plant EGases. Interestingly, this sequence is highly conserved between dicots and monocots. The sequence shows 94% identity between KOR and Cel3, and one rice EST encodes a polypeptide showing 82% identity to this segment in KOR (Figure 4C). KOR, Cel3 and the rice EST are more similar to each other than to other plant EGases suggesting a functional specialization preceding the divergence between monocots and dicots in evolution (Figure 5). KOR and Cel3 also can be distinguished from other EGases by the presence of a C-terminal extension of 30 amino acids rich in prolines (Figure 4A).

KOR is an integral membrane protein

To determine the intracellular localization of KOR, a polyclonal rabbit antiserum was raised against a chimeric protein produced in *Escherichia coli*, composed of bacterial glutathione-S-transferase fused to the 65 N-terminal amino acids of KOR.

Immunoblotting with the immuno-purified antiserum demonstrated the presence of a 70 kDa protein in wild-type leaf microsomes but not in soluble fractions (Figure 6A, lanes 1 and 2). No cross-reacting band was detected in the mutant, demonstrating the specificity of the antiserum (Figure 6A; lanes 3 and 4). After treatment of the microsomes with Na₂CO₃ (pH 11), a procedure known to strip peripheral proteins from membranes, the cross-

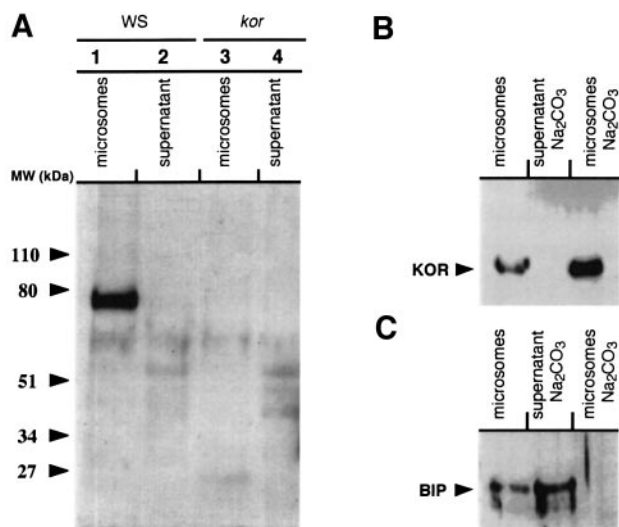


Fig. 6. KOR is an integral membrane protein. (A) Immunoblot of wild-type (lanes 1 and 2) and *kor* (lanes 3 and 4) leaf microsomes (lanes 1 and 3) and supernatant (lanes 2 and 4). (B) Immunoblot of wild-type leaf microsomes before and after Na_2CO_3 (pH 11) extraction. A polyclonal rabbit antiserum raised against the N-terminus of KOR (anti-NKOR) was used in (A) and (B) as primary antibody. (C) Immunoblot of wild-type leaf microsomes before and after Na_2CO_3 (pH 11) extraction, with a polyclonal rabbit antiserum against the soluble ER-localized protein BIP as primary antiserum (Höfte *et al.*, 1992).

reacting protein remained in the membrane fraction (Figure 6B). As a control, the soluble binding protein (BIP), present in the reticulum lumen (Denecke *et al.*, 1993), was recovered in the soluble fraction (Figure 6C). These results show that KOR is an integral membrane protein.

KOR is preferentially located in the plasma membrane

Microsomal membrane vesicles prepared from an *A.thaliana* suspension culture were separated using two consecutive rounds of free-flow electrophoresis (Canut *et al.*, 1988). A first separation yielded three peaks (Figure 7A), respectively enriched for (1) plasma membranes, (2) endoplasmic reticulum (ER) membranes and (3) tonoplast markers. Fractions 1 and 3 were pooled and subjected to a second separation, yielding fractions 4 and 6 (Figure 7B) that were highly enriched for plasma membrane and tonoplast, respectively (Table I). Fraction 2 was also subjected to a further round of purification giving fraction 5 (Figure 7C), which was further enriched for the ER marker. Essentially immunoblotting localized KOR to the plasma membrane-enriched fraction (Figure 7D), no cross-reacting protein was detected in the ER fraction. A faint 70 kDa band could be detected in the tonoplast fraction together with some smaller molecular weight bands. These bands were reproducibly present in different experiments and might be the result of the proteolytic cleavage of the protein in the vacuole.

Cell wall alterations in *kor*

Using microscopy, the walls of mutant and wild-type were investigated on transverse hypocotyl sections of 7-day-old dark-grown seedlings. Transmission electron microscopy (TEM) showed that fixed mutant cell walls were invariably thicker than wild-type walls. This was true both for the

external epidermal wall ($0.9 \pm 0.38 \mu\text{m}$ [$n = 156$] in *kor* versus $0.56 \pm 0.31 \mu\text{m}$ [$n = 162$] in the wild-type) and cortical walls ($0.37 \pm 0.19 \mu\text{m}$ [$n = 10$] in *kor* versus $0.14 \pm 0.05 \mu\text{m}$ [$n = 10$] in the wild-type). The distribution of polysaccharides was visualized by periodic acid-thiocarbohydrazyde-silver proteinate (PATAg) staining (Thiéry, 1967; Roland and Vian, 1991). In epidermal walls three domains could be distinguished including an intensely stained cuticle, a poorly stained outer layer and a strongly stained inner layer. Wild-type walls had a regular surface and visible layers of material could be distinguished in the innermost layer (Figure 8A). In the external epidermal wall of *kor*, the staining was much more irregular, i.e. highly electron-dense deposits were visible at the cytoplasmic side of the wall (see white arrows on Figure 8B), whereas in other areas staining was practically absent. In mutant cortical cell walls irregular fibrillar material could be observed (Figure 8D) compared with the wild-type (Figure 8C).

To visualize cellulosic material, sections were stained with calcofluor (Figure 1G and H). In the wild-type a regular distribution of fluorescent material could be observed in epidermal and cortical cell walls. Separation of cortical walls could be observed occasionally, but exclusively at cell corners. In the mutant, walls of adjacent cortical cells were separated at numerous places distributed over the entire cell surface (Figure 1H, arrows), and the fluorescent staining was more irregular.

Xyloglucan (XG) epitopes were visualized in external epidermal walls with a polyclonal anti-XG antiserum. Gold particles could be observed throughout the wall section for both wild-type and mutant (Figure 8E and F). To assess the contribution of the cellulose-xyloglucan network to the integrity of the wall, an extraction was carried out with the Ca^{2+} -chelator CDTA, a procedure known to selectively extract Ca^{2+} -bridged pectates from the wall (Jauneau *et al.*, 1992). In the wild-type, CDTA extraction caused the wall to swell, but with the preservation of the overall wall structure (Figure 8G). Fibrillar material decorated with antibodies could be seen in the innermost half of the wall. CDTA-treated *kor* mutant walls contained XG in amounts comparable with that observed in the wild-type as indicated by the gold-labeling; however, CDTA not only caused mutant walls to swell, but invariably resulted in the separation of the most recently deposited material from the rest of the wall. Disordered fibrillar material could be observed in the ruptured areas (Figure 8H).

Regulation of KOR-mRNA levels

Northern blot analysis using a probe specific for KOR detected a single transcript of 2 kb in wild-type plants. The mRNA was found in all organs, with the highest levels in stems and roots, and the lowest in siliques (5.5 times less than in stems; Figure 9A and B). Although not visible on Figure 9A, a faint band was also detected in *kor* seedlings and adult plants (Figure 9B).

To investigate a potential role for KOR in the control of cell elongation, KOR-mRNA levels were monitored during hypocotyl development in the dark (Figure 10). No KOR mRNA could be detected in seeds imbibed for 3 h or in 1-day-old seedlings. Hypocotyls started elongating between day 1 and 2 after transfer to the culture room.

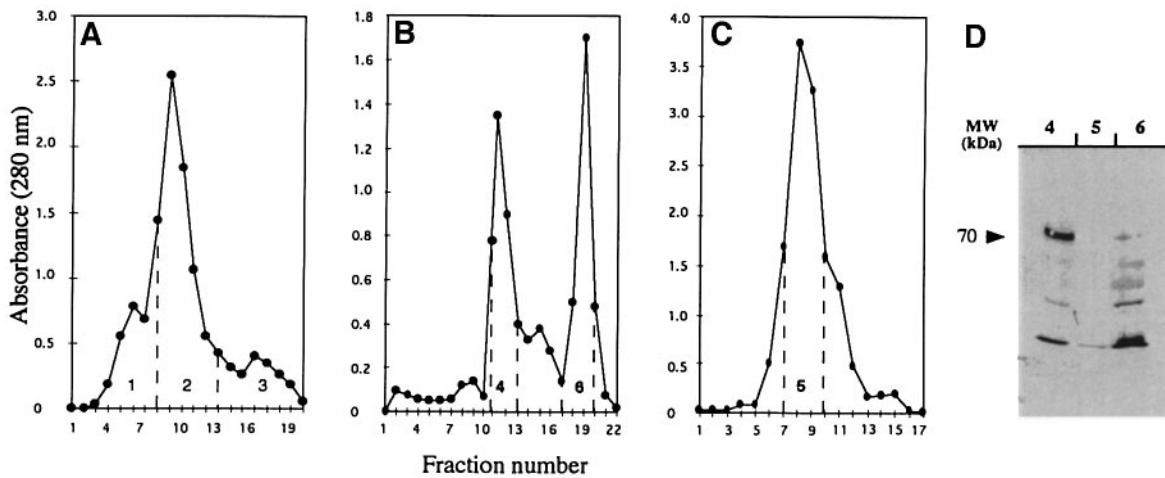


Fig. 7. KOR is primarily located in the plasma membrane. Separation of microsomal membranes by free-flow electrophoresis. (A) Separation profiles of microsomal membranes. (B) Profile obtained after a second separation round of pooled fractions 1 and 3 and (C) after a second separation round of fraction 2. Profiles were monitored at 280 nm. Fractions 4 and 6 are respectively enriched for plasma membrane and tonoplast markers as summarized in Table I. (D) Immunoblot analysis of membrane fractions (50 μ g protein/lane) with the same rabbit anti-NKOR primary antiserum as in Figure 8.

Table I. Enrichment of free-flow electrophoresis fractions for plasma membrane- and tonoplast-associated ATPase activities

	Marker enzymes (fractions)	
	4	6
Total ATPase activity (nmoles Pi/ min.mg protein)	1297	231
Inhibition (%) by KNO_3 (tonoplast)	-1	89
Inhibition (%) by NaN_3 (mitochondria)	1	12
Inhibition (%) by V_2O_5 (plasma membrane)	86	15

Fractions are as in Figure 7.

The growth rate increased between day 2 and 4 after which it dropped (Figure 10A). At day 2, concomitant with the onset of hypocotyl elongation, the mRNA appeared. *KOR*-mRNA levels were highest during the linear growth phase of the hypocotyl (day 4 to 6) and decreased at day 7, at least 1 day, and possibly 2 days, after the drop in growth rate (Figure 10B and C).

Using a set of mutants, we investigated the effect of cell elongation-controlling hormones on the hypocotyl length and *KOR*-mRNA levels of 4-day-old dark-grown seedlings (Figure 11). The mutant *det2* is deficient for an early step of the brassinosteroid biosynthetic pathway (Fujioka *et al.*, 1997). Hypocotyls of *det2* were three times shorter than those of the wild-type. Interestingly, *det2* seedlings showed 3-fold lower *KOR*-mRNA levels than the wild-type. The addition of 10^{-7} M brassinolide (BR) to the medium partially restored hypocotyl growth of *det2* and also caused an increase in *KOR*-mRNA levels. Treatment of wild-type plants with BR caused a slight decrease in length and in *KOR*-mRNA levels (Figure 11A). Seedlings homozygous for the *sur2* mutation contain increased levels of free indolacetic acid (IAA) and reduced levels of conjugated IAA (Delarue *et al.*, 1998). Figure 1 shows that *sur2* hypocotyls were shorter than those of the wild-type. This has been observed previously and reflects the inhibitory effect on elongation of high levels of free

auxin. *KOR*-mRNA levels were ~50% higher in *sur2* compared with the wild-type (Figure 11B); however, this difference was not reproducible in independent experiments (data not shown). Mutant *eto* seedlings overproduce ethylene (Vogel *et al.*, 1998) and show the characteristic triple response of reduced length and increased width of hypocotyl and root, and an exaggerated apical hook. Despite the dramatic differences in hypocotyl length, no significant differences in *KOR*-mRNA levels were observed (Figure 11B). GA treatment (see Materials and methods) of wild-type plants did not affect hypocotyl length and caused a small increase in *KOR*-mRNA levels, which was not reproducible in different experiments. The mutant *gal* (*abc33*) is deficient for the first committed step in GA biosynthesis (Dubreucq *et al.*, 1996) and failed to elongate normally in the presence of low concentrations of GA_{4+7} . Despite the dramatic difference in hypocotyl length, *KOR*-mRNA levels did not differ significantly between *gal* (*abc33*) and wild-type plants (Figure 11C).

Discussion

Our screen yielded a single *KOR* allele whereas multiple alleles were found for other dwarf loci. An explanation for the low allele frequency could be that *kor* is a rare leaky mutation caused by a T-DNA insertion in the promoter, and that the null allele has a more drastic phenotype, not recovered in our screen. In accordance with this, Northern blots of RNA from *kor* revealed a faint band hybridizing to the *KOR* probe, suggesting that residual *KOR* activity may be present in the mutant. Indeed, it is likely that this faint band does not correspond to the mRNA from a related gene, since the same probe did not reveal the presence of a second cross-reacting sequence on low-stringency Southern blots (data not shown).

Despite the usual precautions that need to be taken when deducing a gene function from the phenotype of a single mutant allele, the following observations together indicate that the reduced expression of *KOR* is the primary cause of the growth defect in the mutant. First, the dwarf

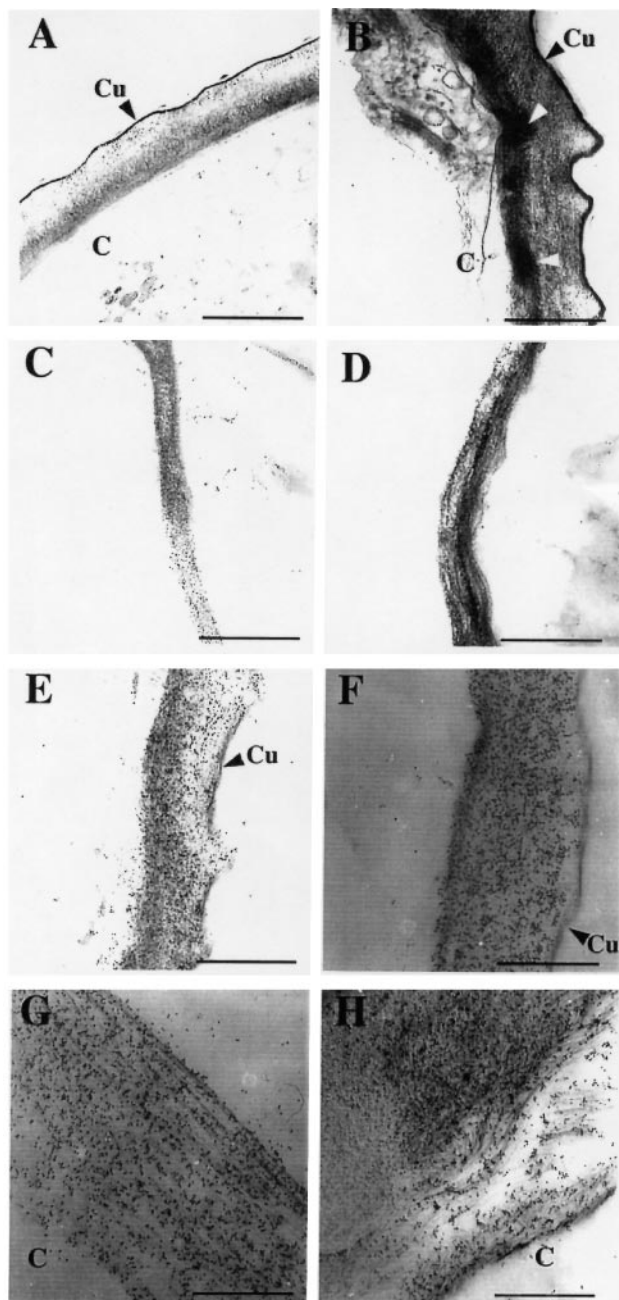


Fig. 8. Cell wall defects in *kor* mutants. Transmission electron microscopy of transverse hypocotyl sections. (A, B) Outer epidermal and (C, D) cortical cell walls sections of 7-day-old dark-grown (A, C) wild-type and (B, D) *korrigan* hypocotyls. Sections were stained for polysaccharides with PATAg. Note the irregular surface and the absence of stratified microfibrils in the inner part of the mutant wall. White arrows indicate aggregates of highly electron-dense material frequently observed at the cytoplasmic side of mutant walls. (E, F, G, H) Outer epidermal sections of 7-day-old dark-grown (E, G) wild-type and (F, H) *korrigan* hypocotyls submitted (G, H) or not (E, F) to a CDTA extraction. Xyloglucans were visualized with polyclonal anti-XG-antibodies and polysaccharides stained by the PATAg method. C, cytoplasm; Cu, cuticle. Scale bar represents 0.6 μ m.

mutant phenotype cosegregated with a T-DNA insertion 200 bp upstream of the initiation codon of *KOR*. Secondly, no major DNA rearrangements surrounding the T-DNA were observed, suggesting that no other genes were inactivated as a result of the T-DNA insertion (data not shown). Thirdly, in the mutant, *KOR*-mRNA and protein

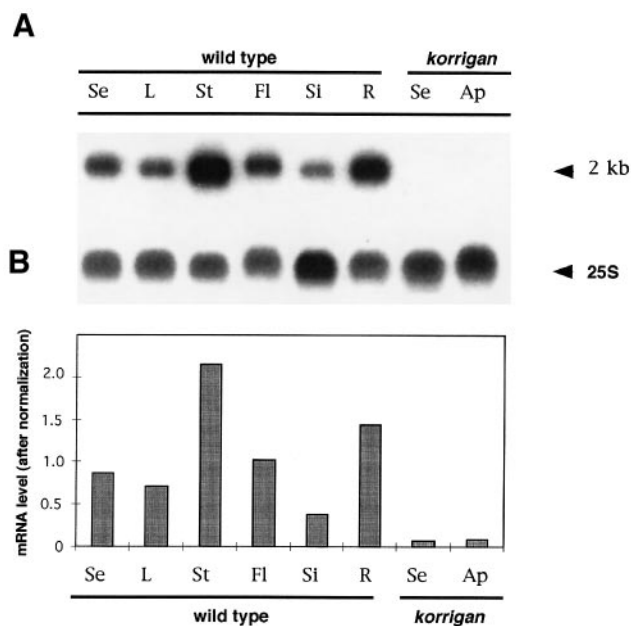


Fig. 9. Ubiquitous expression of *KOR* mRNA. (A) Northern blot with 8 μ g total RNA from wild-type and *kor* tissues: Se, 7-day-old light-grown seedlings; L, leaves; St, stems; Fl, flowers; Si, siliques; R, roots; and Ap, the entire aerial portion of an adult plant, were hybridized with the 765 bp *Pst*I-*Pst*I fragment (between positions 184 and 879 in the *KOR* genomic sequence, see Figure 4). A faint 2 kb transcript was detected with this probe, in *kor* mRNA. (B) Relative quantities of *KOR* mRNA after normalization with the hybridization signal obtained with a 25S RNA gene probe.

levels were strongly reduced, which is consistent with the recessive nature of the mutant phenotype. Fourthly, all aspects of the mutant phenotype were complemented by an ectopically inserted 8.5 kb DNA fragment containing the wild-type *KOR* gene.

Although the enzymatic activity remains to be demonstrated, the following observations suggest that *KOR* encodes a bona fide EGase. The predicted *KOR* sequence is similar to secreted plant EGases over almost its entire length, and the residues essential for catalytic activity in bacterial CelD are conserved. In addition, Brummel *et al.* (1997) observed EGase activity using the artificial substrate CMC in sucrose density/gradient fractions enriched for the tomato ortholog of *KOR*, Cel3. We have also observed membrane-associated CMC-ase activity in *A.thaliana* microsomes (F.Nicol, unpublished data), but it remains to be determined whether this indeed corresponds to the activity of *KOR*.

Whereas almost all other characterized EGase family members in plants and bacteria are soluble secreted enzymes (Brummel *et al.*, 1994), *KOR* and its tomato ortholog Cel3 are unique in that they are both integral membrane proteins. The membrane location was suggested by the presence of a predicted N-terminal transmembrane anchor in the sequence, and was confirmed experimentally for both proteins. Based upon the charge distribution around the transmembrane anchor, the protein is predicted to be a type II membrane protein, with the N-terminus facing the cytosol. This orientation was experimentally confirmed for Cel3, and therefore, in view of the strong sequence conservation (82% amino acid identity), is also likely to be true for *KOR*. Essentially, as for Cel3, *KOR*

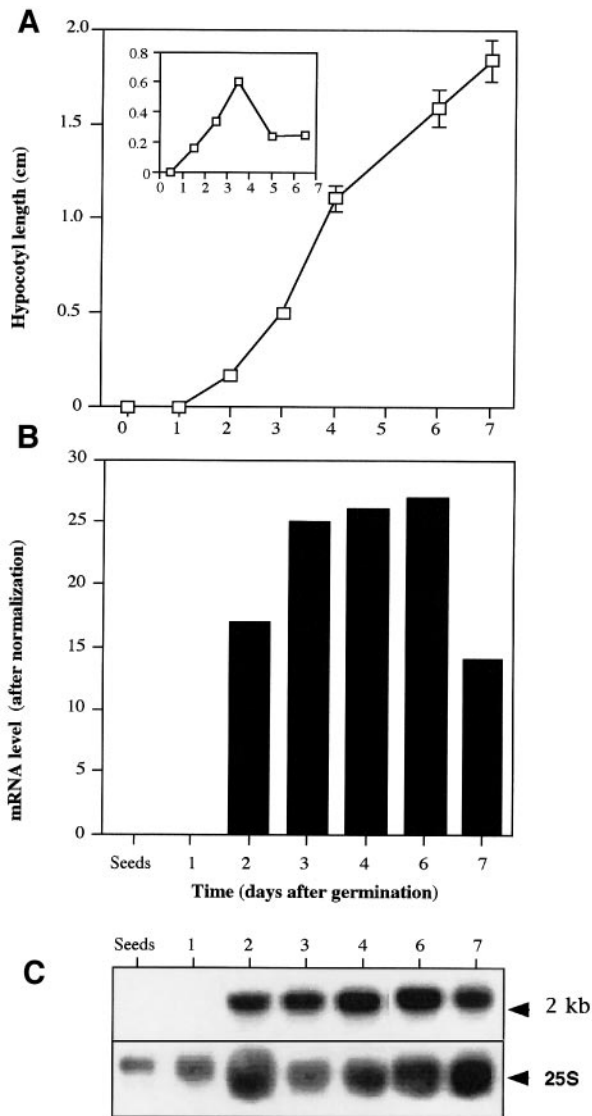


Fig. 10. *KOR* mRNA appears after germination together with the initiation of hypocotyl elongation in the dark. (A) Growth kinetics of wild-type dark-grown hypocotyls and growth rate (inset) in cm/day. (B) Relative quantities of *KOR* mRNA after normalization with the signal from a 25S RNA probe. (C) Northern blot with RNA isolated from seeds imbibed for 3 h and from 1- to 7-day-old dark-grown wild-type seedlings. The same probe as in Figure 9 was used.

was found in the plasma membrane fraction. We also observed a minor portion of KOR in the internal membrane fraction enriched for the tonoplast and different from the ER. Cel3 was also found in internal membranes but in the fraction enriched for the Golgi apparatus. It is not known whether this discrepancy is a result of the different separation procedures used in the two studies (linear sucrose gradient versus free-flow electrophoresis) or reflects differences specific to the two species or the physiology of the tissue investigated (tomato root versus *A.thaliana* suspension cultures). In any case, these data suggest a complex regulation of the intracellular targeting of KOR/Cel3. A detailed localization, together with pulse-chase experiments, are needed to determine exactly in which intracellular compartments the KOR protein resides during the different stages of cellular growth and differentiation.

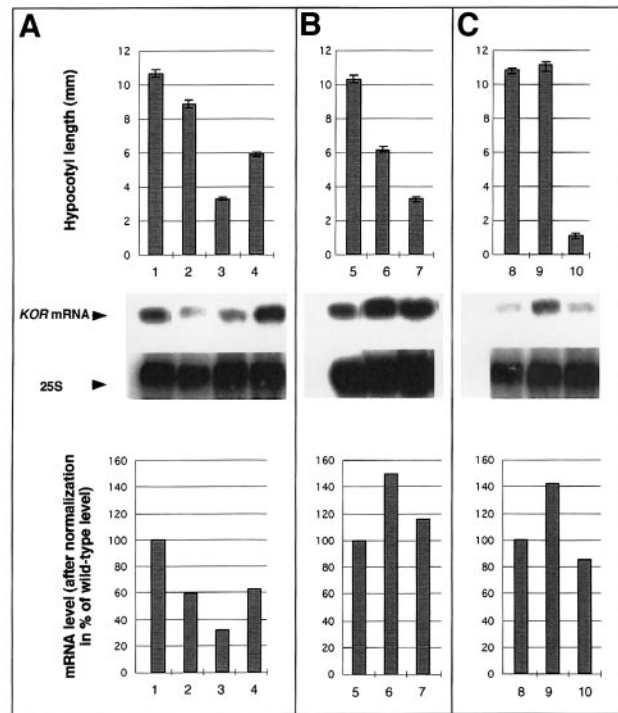


Fig. 11. Effect of cell elongation-controlling hormones on the hypocotyl length of 4-day-old seedlings and on *KOR*-mRNA levels. (A) Effect of brassinosteroids (BR). Wild-type seedlings (Col0 ecotype) non-treated (lane 1) or treated (lane 2) with 10^{-7} M BR. *det2* seedlings non-treated (lane 3) or treated (lane 4) with BR. (B) Wild-type seedlings (Col0 ecotype; lane 5), auxin-overproducing mutant *sur2* (lane 6) and ethylene-overproducing mutant *eto* (lane 7). (C) Effect of GA_{4+7} . Wild-type seedlings (WS ecotype) untreated (lane 8) or treated (lane 9) with 10^{-7} M GA_{4+7} , and *gal* (*abc33*) mutant treated with 10^{-7} M GA_{4+7} (lane 10).

The N-terminal part of KOR, containing the cytosolic domain and the membrane anchor sequence, is highly conserved between rice, tomato and *A.thaliana*. The membrane location therefore appears to be under a strong selective pressure and predates the divergence between monocots and dicots. The membrane location of a cell wall-modifying enzyme may have the following advantages. First, in contrast to soluble secreted proteins, membrane proteins may be more easily targeted to a particular subdomain of the cell wall; for instance, it might be more favorable to express an elongation-promoting enzyme in the longitudinal and not in the transverse wall. Secondly, it may be advantageous to confine the protein to the innermost area of the wall, where it may contribute to the construction of the expanding wall. Thirdly, the regulation of the abundance of the protein in plasma membrane through endo- or exocytosis may be a way to control the amount of enzyme in the wall. In this respect, the observation that a 70 kDa and some smaller cross-reacting bands were present in the tonoplast-enriched fraction might point to a plasma membrane retrieval and vacuolar degradation mechanism. Fourthly, KOR may form part of a complex with other membrane and/or cytosolic proteins. We are currently investigating these different possibilities.

A role for KOR in cell elongation

This study demonstrates, for the first time to our knowledge, an essential role for a member of a family of cell

wall hydrolytic enzymes in normal cell elongation. In the mutant, cell divisions during embryogenesis and in the meristems take place normally (data not shown), suggesting no role for *KOR* in cell plate formation during cytokinesis, although in the absence of a true null allele, this possibility cannot be ruled out entirely. In contrast, the mutant phenotype indicates a role for *KOR* in the elongation of all cells investigated, except for tip-growing cells. The increased diameter of mutant cells, clearly observed in dark-grown hypocotyls, suggests a role for *KOR* in the control of the direction of cell expansion. Increased radial expansion was also observed for the cellulose-deficient mutant *rsw1* (Arioli *et al.*, 1998) or wild-type plants cultured in the presence of cellulose biosynthesis inhibitors, indicating a central role for cellulose in determining the cell shape. As discussed below, the observed cellular phenotype in *kor* would be compatible with a defect in the cellulose-hemicellulose network.

Consistent with the mutant phenotype, *KOR* mRNA was found in all growing organs examined. In the developing hypocotyl, *KOR*-mRNA levels were correlated with cell elongation. The mRNA appeared at the onset of cell elongation in the hypocotyl and reached a maximum during the linear growth phase. Interestingly, the drop in growth rate after the fourth day of culture was not preceded but followed by a drop in *KOR*-mRNA levels, indicating that the growth arrest is not caused by a reduction in *KOR*-mRNA levels.

We did not observe pronounced variations in *KOR*-mRNA levels between the different hormone mutants, except for the brassinosteroid-deficient mutant *det2* in which the reduced hypocotyl length was associated with a modest but reproducible reduction in *KOR* mRNA. It remains to be seen whether *KOR*-mRNA levels are under direct brassinosteroid control, or whether the reduced expression level is an indirect result of reduced cell elongation. Interestingly, the hypocotyl lengths of auxin and ethylene overproducers as well as the GA-deficient mutant were more or less affected without a significant reduction in *KOR* mRNA, suggesting a specific action of BR on *KOR* expression. BR has been shown to regulate the mRNA levels of *TCH4* encoding a xyloglucan-endo-transglycosylase (XET)-homolog (Kauschmann *et al.*, 1996). XETs are thought to be involved in the molecular grafting reactions required for the insertion of new polysaccharides into the cell wall. The mutant phenotype also suggests a similar role for *KOR*. This raises the interesting possibility that growth control by brassinosteroids is mediated through the expression of a set of enzymes involved in the construction of the cell wall. More detailed studies are needed to determine the relationship between hormone action, cell elongation and the expression of *KOR* at the transcriptional but also at different post-transcription levels.

A role for *KOR* in the assembly of the cellulose-hemicellulose network in the primary wall

A number of changes in the architecture of primary walls were observed in *kor*. First, fixed mutant walls were thicker than those of the wild-type. This could be an indirect result of the fixation procedure rather than a true increase in thickness of the unfixed wall. In either case, the results point to an alteration of the physicochemical

properties of *kor* walls. Secondly, polysaccharides were deposited in an irregular fashion in both external epidermal and cortical cell walls. Thirdly, the extraction of the wall with CDTA, a treatment that selectively removes Ca^{2+} -linked acidic pectins, caused a separation of the innermost layers from the rest of the wall, which was never observed in wild-type walls. This interesting observation suggests that, in *kor*, the cellulose-xyloglucan network that remains following removal of the Ca^{2+} -pectate network, is unable to maintain the integrity of the innermost layers of the wall. A similar situation has been observed previously in DCB-adapted tomato cell cultures. In these cells a cellulose-xyloglucan network was practically absent, and Ca^{2+} -linked acidic pectins were required for maintaining the integrity and strength of the wall.

Assuming that *KOR* is an EGase, how could the absence, or the reduced levels of *KOR* cause such changes in the cellulose-XG network? EGases hydrolyse 1,4- β linkages behind unsubstituted glucose residues. Cellulose, xylans and xyloglucans contain 1,4- β linkages. *KOR*, like all known plant EGases, lacks a cellulose-binding domain and would be unable to hydrolyse crystalline cellulose. Xylans mainly accumulate during secondary wall formation, and the absence of a xylanase would not be expected to cause a primary cell wall phenotype. In the current model for the primary wall in dicots, the reduction of xyloglucanase activity would be compatible with reduced wall loosening and cell elongation. In addition, it has been proposed that xyloglucans need to be cleaved in order to permit the incorporation of new microfibrils into the existing cellulose-xyloglucan network (Hayashi, 1989). In this context, the observed unordered accumulation of wall material at the cytoplasmic side of mutant walls and the reduced coherence of the CDTA-extracted walls would be compatible with a reduced ability to cleave load-bearing xyloglucans in the mutant. In this view though, it remains to be explained why a highly conserved *KOR* ortholog is present in rice, since in grasses XGs do not play a predominant role in primary wall structure (Carpita, 1996).

In conclusion, a mutation causing a reduction in the amount of *KOR*, a putative EGase primarily located in the plasma membrane, caused a cell elongation defect in all non-tip-growing cells investigated. In dark-grown hypocotyls, the growth defect is associated with pronounced changes in the cellulose-xyloglucan network within the primary wall. We are currently investigating the substrate specificity of *KOR*, the architecture of mutant walls, and the regulation of the expression and localization of the protein. These studies will further clarify the biochemical, cellular and developmental function of *KOR*, and provide new insights into the molecular mechanisms involved in the construction of the wall and the control of cell elongation in plants.

Materials and methods

Plant strains and growth conditions

Seeds of *A. thaliana* Heyhn, ecotypes Wassilewskija (WS) and Columbia (Col0) were provided by K. Feldman (University of Arizona, Tucson, USA). Mutants used were the GA-deficient mutant *abc33*, allelic to *gal* (Dubreucq *et al.*, 1996; provided by B. Dubreucq), the ethylene-overproducing mutant *eto* (Guzman and Ecker, 1990; provided by ABRC, Columbus, Ohio, USA), the auxin-overproducing mutant *sur2* (Delarue

et al., 1998; provided by C.Bellini) and the brassinosteroid-deficient mutant *cop7*, allelic to *det2* (X.-W.Deng, personal communication; provided by X.-W.Deng). Seeds were sterilized as described by Santoni *et al.* (1994). Seeds were allowed to germinate on nutrient medium as described by Estelle and Somerville (1987) with 1% sucrose, with or without GA₄₊₇ (Sigma) or brassinosteroids (provided by S.Fujioka, RIKEN, Wako-shi, Japan) in a growth chamber. For the GA experiment, seeds were imbibed in a GA₄₊₇ solution (10⁻⁵ M) at 4°C for 48 h and washed five times with sterilized water before being sown on the appropriate medium. Plants were grown in a 16h light (200 μmol/m²/s), 8 h dark cycle. Temperatures were 20 and 15°C, respectively, during day and night. Seeds were imbibed for 48 h at 4°C and exposed to white light (200 μmol/m²/s) before transfer to final growth conditions. For dark conditions, plates were wrapped in two layers of aluminium foil. Days of growth were counted after transfer of Petri dishes from 4°C to the growth chamber. *A.thaliana* suspension cultures were obtained and maintained as described by Axelos *et al.* (1992).

Hypocotyl length measurements

Seedlings (30–40) were spread out on agar plates and magnified using a photographic enlarger. The projected image was traced with a pencil on a sheet of paper. Lengths were measured using image analysis software (Optimas 4.1) as described by Gendreau *et al.* (1997).

Microscopy

SEM and light microscopy were done as described by Desnos *et al.* (1996). *Arabidopsis thaliana* seedlings were fixed, dehydrated and embedded in LR White or Spurr's epoxy medium as described previously (His *et al.*, 1997). Transverse sections (90 nm in thickness) were mounted on gold grids (Ø: 3.05 mm, Oxford Instruments, Orsay, France) and polysaccharides were visualized through PATAg staining (Roland and Vian, 1991). For visualization of XGs in the wall, 7-day-old dark-grown seedlings were fixed with 4% of glutaraldehyde in 0.1 M cacodylate buffer (pH 7.2) at room temperature for 90 min. This treatment was followed by a CDTA-Na₂ extraction at 4°C for 24 h. Seedlings were then submitted to a post-fixation in a solution of 2% (w/v) osmium tetroxide for 1 h. Specimens were then briefly rinsed in deionized water and dehydrated by bathing in graded mixtures of ethanol and water (10, 20, 40, 60, 80, 90, 95 and 100%, v/v). They were bathed in a solution of graded London Resin White (LRW, Oxford Agar)/ethanol (v/2v, v/v, 2v/v) for 30 min each and embedded in LRW overnight at 60°C. Transverse sections (90 nm in thickness) were mounted on gold grids. Samples were then treated in a 3% milk [Tris saline buffer + 0.1% Tween (TTBS)] solution for 30 min. Sections were washed in TTBS buffer and incubated at 4°C for 12 h with a 1:100 dilution of the XG antiserum (Moore *et al.*, 1986). Grids were washed with TTBS buffer and incubated for 1 h with a 1:40 dilution of the secondary goat anti-rabbit antiserum linked to 10 nm gold particles. Grids were then washed for 30 min in TTBS and milliQ water. Polysaccharides were visualized on those sections through PATAg staining.

Isolation of the *korrigan* mutant and genetic analysis

Approximately 12 000 individual T-DNA-mutagenized T₂ lines (Bechtold *et al.*, 1993) and about 800 M₂ families from single ethylmethane sulfonate (EMS) mutagenized M₁ plants (Desnos *et al.*, 1996) were screened for short hypocotyl mutants in the dark. Progeny of putative *kor* heterozygotes (kanamycin resistant seedlings with a wild-type phenotype) were allowed to germinate on non-selective medium and scored for the appearance of the mutant phenotype. The mutant phenotype segregated in a 1:3 ratio in all progeny of all plants tested. Seedlings showing a mutant phenotype were transferred to a selective medium. All the phenotypically mutant seedlings (800) showed resistance to kanamycin, indicating a tight linkage between the inserted T-DNA and the mutant phenotype (<3 cM).

Southern and Northern blot analysis

Arabidopsis thaliana genomic DNA was isolated as previously described (Bouchez *et al.*, 1996). For RNA extraction, tissues from different parts of 4- to 5-week-old wild-type (WS) plants were harvested and immediately frozen in liquid nitrogen. For root-RNA preparations, plants were grown in liquid culture medium (described in Estelle and Somerville, 1987; but without agarose) for 15 days then harvested and frozen in liquid nitrogen. For expression kinetics, seedlings were grown in the dark in Petri dishes containing medium covered by filter paper, then harvested at the appropriate day under a green safe light and frozen in liquid nitrogen. Seeds were imbibed in water for 3 h and frozen. RNA was extracted as described by Sambrook *et al.* (1989). Southern and

Northern blots were performed using Hybond N membranes and hybridized to random primed probes following the manufacturer's instructions (Amersham, Buckinghamshire, UK). Northern blots were carried out with a 765 bp *PstI*-*PstI* fragment from the genomic clone as a probe. For the hormone experiment, the Northern blot was hybridized with the 273 bp *BglIII*-*BglIII* cDNA fragment as a probe.

Molecular cloning of the *KORRIGAN* gene

Standard molecular cloning techniques were performed as described by Sambrook *et al.* (1989). Southern blot analysis revealed the presence of a single T-DNA insertion. Genomic DNA of the *korrigan* mutant was digested by *MspI* and ligated with T4-DNA ligase. A right border flanking sequence was obtained through Inverse Polymerase Chain Reaction (IPCR) using the method described by Lindsey and Topping (1996). The PCR reaction was performed using the T-DNA oligonucleotides TAG7 (5'-GGACTGACCACCCCAAGTGC-3') and TAG8 (5'-ACTCGACGGCCTGTGGGCAT-3'). The 600 bp flanking fragment was used to probe an *A.thaliana* genomic phage library made by John Mulligan and distributed via the EEC-BRIDGE *Arabidopsis* DNA Stock Center. A positive phage clone was digested with *PstI* and subcloned into the pZero vector (Invitrogen, Leek, The Netherlands). DNA sequencing was performed using an ABI 373A automated sequencer (Applied Biosystems). A 8.5 kb *XhoI* DNA fragment presumed to contain the entire *KORRIGAN* gene was introduced into the *XhoI* site of the binary vector pBIB-HYG (Becker, 1990) containing a hygromycin resistance marker. The recombinant binary vector was introduced into *Agrobacterium* strain C58C1 (pMP90; Koncz and Schell, 1986) through electroporation. The T-DNA was transformed into plants heterozygous and homozygous for *korrigan* using the infiltration protocol described by Bechtold *et al.* (1993). Transformants were selected *in vitro*, on a medium containing hygromycin (100 μg/ml). The F₂ progeny of individual hygromycin resistant plants were analyzed for the segregation of *korrigan* mutants. A cDNA library (D'Alessio, 1992) was also screened with the 765 bp *PstI*-*PstI* genomic fragment. The *KORRIGAN* predicted amino acid sequence was used to search the protein sequence databases using the programs BLASTX and TBLASTN (Altschul *et al.*, 1990). Endo-1,4-β-D-glucanases were aligned using the Pileup program within the GCG program package, version 9.0 (Genetics Computer Group). Identical amino acids were visualized using the program SeqVu, version 1.1 (Garvan Institute, Sydney, Australia).

Mapping

PCR screening of the CIC library was performed as described by Creusot *et al.* (1995) using ordered YACs pooled in three dimensions. Two oligonucleotides, B (5'-GAGACGCAGCAGAGTTGGTT-3') and C (5'-AGATCATCAATGGAATCAGCAG-3'), the 5' ends of which respectively correspond to nucleotides 194 and 744 of the *KOR* cDNA sequence, were used to amplify by PCR a unique 550 bp fragment from genomic *A.thaliana* Columbia DNA. The PCR primers identified two YAC clones (CIC 4G5 and CIC 8D5) located at the bottom of chromosome V and containing the microsatellite marker nga129 (Lister and Dean, 1994) which mapped the gene to chromosome V, position 81.7 cM.

Protein expression and immunological techniques

A cDNA fragment encoding the 65 N-terminal amino acids (NKOR; *NcoI*/86-*BglII*/279) was cloned into pGEX2T6 (Pharmacia) in frame with the glutathion S-transferase (GST) protein. The expression and the purification of the fusion GST-NKOR protein was performed using the recommendations of the manufacturer. The 37 kDa soluble purified recombinant protein was used to produce a rabbit antiserum following the standard immunization protocols of Eurogentec (Seraing, Belgium). The antiserum was purified according to the procedure described by Lin *et al.* (1989). Immunoblots were carried out with a 1:500 dilution of the NKOR rabbit antiserum or a 1:10 000 dilution of the anti-BIP rabbit antiserum (Höfte *et al.*, 1992) and a secondary anti-rabbit IgG F(ab')₂ fragment linked to horseradish peroxidase, according to the specification of the manufacturer (Amersham) on Hybond C membranes (Amersham). Signals were revealed using the Amersham ECL System.

Microsome preparation

Microsomes were prepared from freshly harvested leaves of 6-week-old plants. Tissues (500 mg fresh weight) were ground in 2.5 ml extraction buffer (12% w/w sucrose, 50 mM Tris-HCl pH 7.8, 1 mM EDTA, 1 mM DTT, 0.04 mM leupeptine, 0.02 mM lepeptatine, 1 mg/ml polyvinylpyrrolidone) and centrifuged at 3000 g for 10 min to remove cell walls and debris. The supernatant was layered over 1 ml of 16% (w/w) sucrose and microsomes were pelleted from the supernatant

through centrifugation for 60 min at 35 000 r.p.m. in a TST 55 rotor (Kontron instruments) at 4°C. The supernatant was TCA-precipitated and resuspended in the buffer described above. To strip peripheral proteins from microsomes, the pellet was resuspended in 50 mM Tris with protease inhibitors and adjusted to 100 mM Na₂CO₃ (pH 11.5). Membranes were pelleted from the supernatant through centrifugation for 60 min at 40 000 r.p.m. in a TST 55 rotor (Kontron instrument) at 4°C. The pellet was resuspended in 100 mM Na₂CO₃ (pH 11.5) and centrifuged again. The pellet was resuspended in extraction buffer and the supernatant combined and TCA precipitated. Proteins were quantified using the protein assay kit according to the specification of the manufacturer (Sigma Diagnostics, St Louis, USA) using bovine serum albumin as standard.

Free-flow electrophoresis

Membrane preparation and free-flow electrophoresis were performed exactly as described previously by Canut *et al.* (1988). The specific activities of marker enzymes were determined as described previously (Canut *et al.*, 1990).

Acknowledgements

The authors thank Thierry Desprez for assistance with sequence comparisons; Christine Camilleri and Sophie Desloire for the mapping of the *KOR* locus; Madeleine Lemain, Anne-Marie Jaunet, Brigitte Gelie for SEM; Claude Pethe for assistance with the biochemical techniques; Catherine Bellini, Nicole Bechtold and Georges Pelletier for generating the T-DNA insertion lines and providing assistance in the mutant screen; Jacques Goujeaud and Joël Talbotec for the assistance in the greenhouse; Xing-Wang Deng, Catherine Bellini and Bertrand Dubreucq for kindly providing the mutants *cop7*, *sur2* and *gal1* (*abc33*), respectively; the *Arabidopsis* Biological Resource Center for providing us *eto* seeds and genomic and cDNA libraries; Andrew Staehelin for the anti-XG antibody; Michel Caboche, Jan Traas, Gwenaelle Joliff, Bernard Henrissat, Pierre Beguin for stimulating discussions and Heather McKhann, Michel Caboche and Ageeth van Tuinen for the critical reading of the manuscript. This work was supported by a grant from the Ministère de la Recherche et de la Technologie to F.N., and grant ACC-SV No. 9501006 from the Ministère de la Recherche et de la Technologie to H.H.

References

- Albersheim, P. (1975) The walls of growing plant cells. *Sci. Am.*, **232**, 80–95.
- Altschul, S.F., Gish, W., Miller, W., Myers, E.W. and Lipman, D.J. (1990) Basic local alignment search tool. *J. Mol. Biol.*, **215**, 403–410.
- Arioli, T. *et al.* (1998) Molecular analysis of cellulose biosynthesis in *Arabidopsis*. *Science*, **279**, 717–720.
- Axelos, M., Curie, C., Mazzolini, L., Bardet, C. and Lescure, B. (1992) A protocol for transient gene expression in *Arabidopsis thaliana* protoplasts isolated from cell suspension cultures. *Plant Physiol. Biochem.*, **30**, 123–128.
- Bechtold, N., Ellis, J. and Pelletier, G. (1993) *In planta Agrobacterium* mediated gene transfer by infiltration of adult *Arabidopsis thaliana* plants. *C.R. Acad. Sci. Paris*, **316**, 1194–1199.
- Becker, D. (1990) Binary vector which allow the exchange of plant selectable markers and reporter genes. *Nucleic Acids Res.*, **18**, 203.
- Bouchez, D., Vittorioso, P., Courtial, B. and Camilleri, C. (1996) Kanamycin rescue: a simple technique for the recovery of T-DNA flanking sequence. *Plant Mol. Biol. Rep.*, **14**, 115–123.
- Brummell, D.A., Lashbrook, C.C. and Bennett, A.B. (1994) Plant endo-1,4-β-D-glucanases. Structure, properties and physiological function. In Himmel, M.E., Baker, J.O. and Overend, R.P. (eds), *Enzymatic Conversion of Biomass for Fuels Production*. American Chemical Society, Washington DC, pp. 100–129.
- Brummell, D.A., Catala, C., Lashbrook, C.C. and Bennett, A.B. (1997) A membrane-anchored E-type endo-1,4-β-glucanase is localized on Golgi and plasma membranes of higher plants. *Proc. Natl Acad. Sci. USA*, **94**, 4794–4799.
- Canut, H., Brightman, A., Boudet, A.M. and Morré, D.J. (1988) Plasma membrane vesicles of opposite sidedness from soybean hypocotyls by preparative free-flow electrophoresis. *Plant Physiol.*, **86**, 631–637.
- Canut, H., Brightman, A., Boudet, A.M. and Morré, D.J. (1990) Tonoplast vesicles of opposite sidedness from soybean hypocotyls by preparative free-flow electrophoresis. *Plant Physiol.*, **94**, 1149–1156.
- Carpita, N.C. (1996) Structure and biogenesis of the cell walls of grasses. *Annu. Rev. Plant Physiol.*, **47**, 445–476.
- Carpita, N.C. and Gibeaut, D.M. (1993) Structural models of primary cell walls in flowering plants: consistency of molecular structure with the physical properties of the walls during growth. *Plant J.*, **3**, 1–30.
- Cass, L.G., Kirven, K.A. and Christoffersen, R.E. (1990) Isolation and characterization of a cellulase gene family member expressed during avocado fruit ripening. *Mol. Gen. Genet.*, **223**, 76–86.
- Chauvaux, S., Béguin, P. and Aubert, J.-P. (1992) Site-directed mutagenesis of essential carboxylic residues in *Clostridium thermocellum* endoglucanase CelD. *J. Biol. Chem.*, **267**, 4472–4478.
- Cleland, R. (1971) Cell wall extension. *Annu. Rev. Plant Physiol.*, **22**, 197–222.
- Cosgrove, D.J. (1997) Relaxation in a high-stress environment: The molecular bases of extensible cell walls and cell enlargement. *Plant Cell*, **9**, 1031–1041.
- Creusot, F. *et al.* (1995) The CIC library: a large insert YAC library for genome mapping in *Arabidopsis thaliana*. *Plant J.*, **8**, 763–770.
- D'Alessio, J.M. (1992) Automatic subcloning of cDNA. *Focus*, **14**, 76–79.
- Delarue, M., Prinsen, E., Van Onckelen, H., Caboche, M. and Bellini, C. (1998) *Sur2* mutations of *Arabidopsis thaliana* define a new locus involved in the control of auxin homeostasis. *Plant J.*, **14**, 603–611.
- Del Campillo, E. and Bennett, A.B. (1996) Pedicel breakstrength and cellulase gene expression during tomato flower abscission. *Plant Physiol.*, **111**, 813–820.
- Denecke, J., Ek, B., Caspers, M., Sinjorgo, K.M.C. and Palva, E.T. (1993) Analysis of sorting signals responsible for the accumulation of soluble reticuloplasmins in the plant endoplasmic reticulum. *J. Exp. Bot.*, **44**, 213–221.
- Desnos, T., Orbovic, V., Bellini, C., Kronenberger, J., Caboche, M., Traas, J. and Höfte, H. (1996) *Procuste1* mutants identify two distinct genetic pathways controlling hypocotyl cell elongation, respectively in dark- and light-grown *Arabidopsis* seedlings. *Development*, **122**, 683–693.
- Dubreucq, B., Grappin, P. and Caboche, M. (1996) A new method for the identification and isolation of genes essential for *Arabidopsis thaliana* seed germination. *Mol. Gen. Genet.*, **252**, 42–50.
- Estelle, M.A. and Somerville, C. (1987) Auxin-resistant mutants of *Arabidopsis thaliana* with an altered morphology. *Mol. Gen. Genet.*, **206**, 200–206.
- Ferrarese, L., Trainotti, L., Moretto, P., Polverino de Lauro, P., Rascio, N. and Casadoro, G. (1995) Differential ethylene-inducible expression of cellulase in pepper plants. *Plant Mol. Biol.*, **29**, 735–747.
- Fujioka, S. *et al.* (1997) The *Arabidopsis deetiolated2* mutant is blocked early in brassinosteroid biosynthesis. *Plant Cell*, **9**, 1951–1962.
- Gendreau, E., Traas, J., Desnos, T., Grandjean, O., Caboche, M. and Höfte, H. (1997) Cellular basis of hypocotyl growth in *Arabidopsis thaliana*. *Plant Physiol.*, **114**, 295–305.
- Guzman, P. and Ecker, J.R. (1990) Exploiting the triple response of *Arabidopsis* to identify ethylene-related mutants. *Plant Cell*, **2**, 513–523.
- Hayashi, T. (1989) Xyloglucans in the primary cell wall. *Annu. Rev. Plant Physiol. Plant Mol. Biol.*, **40**, 139–168.
- Hayashi, T. and Maclachlan, G. (1984) Pea xyloglucan and cellulose. I. Macromolecular organization. *Plant Physiol.*, **75**, 596–604.
- Henrissat, B., Claeysens, M., Tomme, P., Lemesle, L. and Mornon, J.-P. (1989) Cellulase families revealed by hydrophobic cluster analysis. *Gene*, **81**, 83–95.
- His, I., Driowich, A. and Jauneau, A. (1997) Distribution of cell wall polysaccharides in the epidermis of flax hypocotyl seedlings: calcium induced-acidification of pectins. *Plant Physiol. Biochem.*, **35**, 631–644.
- Höfte, H. and Chrispeels, M.J. (1992) Protein sorting to the vacuolar membrane. *Plant Cell*, **4**, 995–1004.
- Hoson, T. and Nevins, D.J. (1989) β-D-glucan antibodies inhibit auxin-induced elongation and changes in the cell wall of *Zea* coleoptile segments. *Plant Physiol.*, **90**, 1353–1358.
- Inoué, M. and Nevins, D.J. (1991) Inhibition of auxin-induced cell elongation of maize coleoptiles by antibodies specific for cell wall glucanases. *Plant Physiol.*, **96**, 426–431.
- Jauneau, A., Morvan, C., Lefebvre, F., Demarty, M., Ripoll, C. and Thellier, M. (1992) Differential extractability of calcium and pectin substances in different wall regions of epicotyl cells in young flax plants. *J. Histochem. Cytochem.*, **40**, 1183–1189.
- Kauschmann, A., Jessop, A., Koncz, C., Szekeres, M., Willmitzer, L. and Altmann, T. (1996) Genetic evidence for an essential role of brassinosteroids in plant development. *Plant J.*, **9**, 701–713.

- Koncz,C. and Schell,J. (1986) The promoter of TL-DNA gene controls the tissue-specific expression of chimaeric genes carried by a novel type of *Agrobacterium tumefaciens*. *Mol. Gen. Genet.*, **204**, 383–396.
- Kyte,J. and Doolittle,R.F. (1982) A simple method for displaying the hydropathic character of a protein. *J. Mol. Biol.*, **157**, 105–132.
- Lashbrook,C.C., Gonzalez-Bosch,C. and Benett,A.B. (1994) Two divergent endo- β -1,4-glucanase genes exhibit overlapping expression in ripening fruit and abscising flowers. *Plant Cell*, **6**, 1485–1493.
- Lin,M., Turpin,D.H. and Plaxton,W.C. (1989) Pyruvate kinase isozymes from the green alga, *Selenastrum minutum*. *Arch. Biochem. Biophys.*, **269**, 219–227.
- Lindsey,K. and Topping,J.F. (1996) T-DNA-mediated insertional mutagenesis. In Foster,G.D. and Twell,D. (eds), *Plant Gene Isolation. Principles and Practice*. Wiley, Chichester, UK, pp. 275–300.
- Lister,C. and Dean,C. (1994) Recombinant inbred lines for mapping RFLP and phenotypic markers in *Arabidopsis thaliana*. In *4th International Congress of Plant Molecular Biology*. The International Society for Molecular Biology.
- McCann,M.C., Wells,B. and Roberts,K. (1990) Direct visualization of cross-links in the primary plant cell wall. *J. Cell Sci.*, **96**, 3223–3334.
- Moore,P.J., Darvill,A.G., Albersheim,P. and Staehelin,L.A. (1986) Immunogold localization of xyloglucan and rhamnogalacturonan 1 in the cell wall of suspension-cultured sycamore cells. *Plant Physiol.*, **82**, 787–794.
- Pear,J.R., Kawagoe,Y., Schreckengost,W.E., Delmer,D.P. and Stalker,D.M. (1996) Higher plants contain homologs of the bacterial *celA* genes encoding the catalytic subunit of cellulose synthase. *Proc. Natl Acad. Sci. USA*, **93**, 12637–12642.
- Roland,J.C. and Vian,B. (1991) General preparation and staining of thin sections. In Hall,J.L. and Hawes,C. (eds) *Electron Microscopy of Plant Cells*. Academic Press, London, UK, pp. 1–66.
- Sambrook,J., Fritsch,E.F. and Maniatis,T. (1989) *Molecular Cloning: a Laboratory Manual*. Cold Spring Harbor Laboratory Press, Cold Spring Harbour, NY.
- Santoni,V., Bellini,C. and Caboche,M. (1994) Use of two-dimensional protein-pattern analysis for the characterization of *Arabidopsis thaliana* mutants. *Planta*, **192**, 557–566.
- Staehelin,L.A. and Moore,I. (1995) The plant golgi apparatus: structure, functional organization and trafficking mechanisms. *Annu. Rev. Plant. Physiol. Plant Mol. Biol.*, **46**, 261–288.
- Thiéry,J.-P. (1967) Mise en évidence des polysaccharides sur coupes fines en microscopie électronique. *J. Microscopy*, **6**, 987–1018.
- Tucker,M.L. and Milligan,S.B. (1991) Sequence analysis and comparison of avocado fruit and bean abscission cellulases. *Plant Physiol.*, **95**, 928–933.
- Vogel,J.P., Woeste,K.E., Theologis,A. and Kieber,J.J. (1998) Recessive and dominant mutations in the ethylene biosynthetic gene *ACS5* of *Arabidopsis* confer cytokinin insensitivity and ethylene overproduction, respectively. *Proc. Natl Acad. Sci. USA*, **95**, 4766–4771.
- Von Heijne,G. (1986) A new method for predicting signal sequence cleavage sites. *Nucleic Acids Res.*, **14**, 4683–4690.
- Wu,S.C., Blumer,J.M., Darvill,A.G. and Albersheim,P. (1996) Characterization of an endo- β -1,4-glucanase gene induced by auxin in elongating pea epicotyls. *Plant Physiol.*, **110**, 163–170.

Received September 12, 1997; revised July 2, 1998;
accepted August 11, 1998